THE UNIVERSITY OF READING

Topographical scattering of gravity waves.

by

J.W. Miles & P.G. Chamberlain

Applied Mathematics Report 97/3

DEPARTMENT OF MATHEMATICS

Topographical scattering of gravity waves

By J.W. Miles[1] and P.G. Chamberlain[2]

[1]Institute of Geophysics and Planetary Physics,
University of California, San Diego, La Jolla, California 92093-0225

[2]Department of Mathematics, The University of Reading,
P.O. Box 220, Whitenights, Reading, RG6 6AX, UK

A systematic hierarchy of partial differential equations for linear gravity waves in water of variable depth is developed through the expansion of the average Lagrangian in powers of $|\nabla h|$ (h = depth, ∇h = slope). The first and second members of this hierarchy, the Helmholtz and conventional mild-slope equations, are second-order. The third member is fourth-order but may be approximated by Chamberlain & Porter's (1995) 'modified mild-slope' equation, which is second-order and comprises terms in $\nabla^2 h$ and $(\nabla h)^2$ that are absent from the mild-slope equation. Approximate solutions of the mild-slope and modified mild-slope equations for topographical scattering are determined through an iterative sequence, starting from a geometrical-optics approximation (which neglects reflection), through a *quasi-geometrical-optics* approximation, and on to higher-order results. The resulting reflection coefficient for a ramp of uniform slope is compared with the results of numerical integrations of each of the mild-slope equation (Booij 1983), the modified mild-slope equation (Porter & Staziker 1995), and the full linear equations (Booij 1983). Also considered is a sinusoidal ripple bed, for which Bragg resonance may yield rather strong reflection and for which the modified mild-slope approximation proves effective.

1. Introduction

Linear gravity waves of velocity potential ϕ, free-surface displacement ζ (projected on $z=0$), and frequency ω in water of ambient depth $h(\mathbf{x})$ are described by

$$[\phi(\mathbf{x},z,t),\zeta(\mathbf{x},t)] = \mathrm{Re}\{[\Phi(\mathbf{x},z),\mathrm{i}(\omega/g)\Phi(\mathbf{x},0)]e^{-\mathrm{i}\omega t}\}\,, \tag{1.1}$$

where the complex potential Φ satisfies

$$\nabla^2\Phi + \Phi_{zz} = 0 \quad (-h < z < 0)\,, \tag{1.2}$$

$$\Phi_z = \kappa\Phi \quad (z=0)\,, \quad \kappa \equiv \omega^2/g\,, \tag{1.3a,b}$$

$$\Phi_z + \nabla h\cdot\nabla\Phi = 0 \quad (z=-h)\,, \tag{1.4}$$

$$\mathbf{x} \equiv (x,y)\,, \quad \nabla \equiv (\partial_x,\partial_y)\,, \quad \nabla^2 \equiv \partial_x^2 + \partial_y^2\,. \tag{1.5a-c}$$

Appropriate lateral boundary conditions are implicit.

1.1 The classical problem

If the variation in depth is neglected (1.2)–(1.4) admit the solution

$$\Phi(\mathbf{x},z) = \Phi_0(\mathbf{x})(\cosh kz + \kappa k^{-1}\sinh kz)\,, \tag{1.6}$$

where k is determined by the dispersion relation

$$k\tanh kh = \kappa\,, \tag{1.7}$$

and $\Phi_0(\mathbf{x}) \equiv \Phi(\mathbf{x},0)$ satisfies the Helmholtz equation

$$(\nabla^2 + k^2)\Phi_0 = 0 \quad (k = \text{constant})\,. \tag{1.8}$$

1.2 The mild-slope equation

If $k = k(\mathbf{x})$ is determined by (1.7) with $h = h(\mathbf{x})$ therein and the z-dependence of Φ is approximated by (1.6) in an appropriate averaging procedure [see Smith & Sprinks (1975) or Mei (1983), §3.5] $\Phi_0(\mathbf{x})$ is found to satisfy the 'mild-slope equation'

$$\nabla\cdot(H\nabla\Phi_0) + k^2 H\Phi_0 = 0\,, \tag{1.9}$$

where $$kH = \tfrac{1}{2}[T + kh(1 - T^2)] \quad (T \equiv \tanh kh) \tag{1.10}$$

is a dimensionless group velocity that approximates $kh \simeq (\kappa h)^{1/2}$ for $kh \ll 1$, has a maximum of $\tfrac{1}{2}kh$ at $kh = 1.200$ ($\kappa h = 1$), and then decreases to $\tfrac{1}{2}$ as $kh \uparrow \infty$. The mild-slope equation reduces to the conventional shallow-water equation in the limit $\kappa h \downarrow 0$ ($H \to h$, $k^2 H \to \kappa$) and to the Helmholtz equation (1.8) in the limit $\kappa h \uparrow \infty$ (after division by $H \sim 1/2\kappa$).

We remark that (1.9) implies

$$(\nabla^2 + k^2)\Phi_0 = -H^{-1}\nabla H \cdot \nabla \Phi_0 = O(\varepsilon k^2 \Phi_0)\,, \tag{1.11}$$

where $$\varepsilon \equiv \sigma/kh\,, \quad \sigma \equiv |\nabla h|\,, \tag{1.12a,b}$$

so that the error implicit in the neglect of the variation of depth in (1.8) is $O(\varepsilon)$. It follows from the analysis of Smith & Sprinks (1975) that the error in the accommodation of variable depth in the mild-slope equation (1.9) is $O(\varepsilon^2)$, which is $O(\sigma^2)$ for $kh = O(1)$ but appears to diverge in the shallow-water limit $kh \downarrow 0$; however, it then is more appropriate to introduce $\ell \equiv h/\sigma$ to obtain $\varepsilon = 1/k\ell$. See Mei (1983), §§3.5 and 4.1.1 for further discussion.

1.3 The modified mild-slope equation

Chamberlain & Porter (1995, hereinafter CP), starting from a variational integral that is equivalent to an average Lagrangian (see §2.2) based on the trial function (1.6), derive the 'modified mild-slope equation'

$$\nabla \cdot (H \nabla \Phi_0) + (k^2 H - K)\Phi_0 = 0\,, \tag{1.13}$$

where $$K = K_1(kh)\nabla^2 h + kK_2(kh)(\nabla h)^2\,, \tag{1.14a}$$

$$K_1 = \tfrac{1}{4}(1 - T^2)\left[\frac{kh(1+T^2) - T}{kh(1-T^2) + T}\right] \quad (T \equiv \tanh kh)\,, \tag{1.14b}$$

and $$K_2 = -(1-T^2)\,[kh\,(1-T^2)+T]^{-3}\,\{\tfrac{1}{4}(1-2T^2+3T^4)[(kh)^2(1-T^2)+2khT] + \tfrac{1}{6}\,(kh)^4(1-T^2)^3+\tfrac{2}{3}(kh)^3T(1-T^2)^2-\tfrac{3}{4}T^2(1+T^2)\}\,, \tag{1.14c}$$

($H \equiv u_0$, $K \equiv -r$, $K_1 \equiv -u_1$ and $kK_2 \equiv -u_2$ in CP's notation). The error in the trial function (1.6) is $O(\varepsilon)$, which, if ∇h is continuous, implies an $O(\varepsilon^2)$ error in (1.13) by virtue of the variational principle. It therefore appears that the retention of K, which is $O(\varepsilon^2)$, is inconsistent with (1.6); however, CP and Porter & Straziker (1995) offer examples that strongly support this retention. Moreover, if ∇h is discontinuous the term $K_1\nabla^2 h$ implies an $O(\varepsilon)$ effect, and it follows from the integration of (1.13) across such a discontinuity that (the complex amplitude of) the velocity must satisfy the jump condition (Porter & Staziker 1995)

$$H\,[\nabla\Phi_0] = K_1[\nabla h\,]\Phi_0\,, \tag{1.15}$$

where $$[f\,(x)] \equiv f\,(x+) - f\,(x-)\,. \tag{1.16}$$

But note that the solution of the mild-slope equation (1.9) must satisfy $[\nabla\Phi_0] = 0$ at a discontinuity in ∇h .

1.4. The mild-slope hierarchy

We consider in §2 the expansion of the average Lagrangian in powers of σ to construct a systematic hierarchy of partial differential equations for Φ_0, in which (1.8) and (1.9) are the first and second members. The next member is of fourth order but may be reduced to the modified mild-slope equation (1.13) through an approximaton that is implicit in CP and explicit in the present development.

In §3, we consider extensions of the geometrical-optics approximation (Keller 1958) at levels equivalent to those of the above hierarchy and transform the governing differential equation to a Volterra integral equation. In §4, we apply the development of

§3 to the topographical reflection of a straight-crested wave by a finite interval of variable depth on the assumption that $h(x)$, but not necessarily dh/dx, is continuous and obtain first- and second-order (in σ) analytical approximations to the reflection coefficient through an iterative solution of the integral equation. We also construct a variational form for the reflection coefficient, which is stationary with respect to first-order variations about the solution of the integral equation, and an *ad hoc* approximation based on an interpolation of the wave amplitude over the interval of variable depth.

We compare these approximations with those obtained through the numerical solution of the Volterra integral equation and with results given by others. Two test problems are considered: a linear ramp and a finite patch of small amplitude ripples. Both problems have been discussed elsewhere, and data for comparison are readily available.

2. The average Lagrangian

The specific Lagrangian for the gravity wave described by (1.1)—(1.5) is given by

$$L = \tfrac{1}{2}\iint\left[\int_{-h}^{0}(\nabla\phi)^2 dz - g\zeta^2\right]dxdy\,. \tag{2.1}$$

Substituting ϕ and ζ from (1.1), averaging L over the period $2\pi/\omega$, and invoking $\kappa \equiv \omega^2/g$, we obtain the average Lagrangian

$$\bar{L} \equiv \frac{\omega}{2\pi}\int_0^{2\pi/\omega} L dt = \tfrac{1}{4}\iint \mathsf{L} dxdy\,, \tag{2.2}$$

where

$$\mathsf{L} = \int_{-h}^{0}[\,|\nabla\Phi|^2 + |\Phi_z|^2]dz - \kappa|\Phi_0|^2\,. \tag{2.3}$$

2.1 Operational expansion

We pose the solution of (1.2) and (1.3a) in the form (Miles 1985)

$$\Phi(\mathbf{x},z) = (\cosh\mathsf{k}z + \kappa\mathsf{k}^{-1}\sinh\mathsf{k}z)\Phi_0(\mathbf{x}) \equiv \mathsf{F}(\mathsf{k}^2,z)\Phi_0(\mathbf{x})\,,\quad \mathsf{k}^2 \equiv -\nabla^2\,, \tag{2.4a,b}$$

where the operators $\cosh\mathsf{k}z$ and $\mathsf{k}^{-1}\sinh\mathsf{k}z$ are defined by their power-series expansions in k^2 (note that (2.4a) reduces to (1.6) for $\mathsf{k} = k$), and expand the operator F in powers of the Helmholtz operator

$$\mathsf{H} \equiv \nabla^2 + k^2 = -(\mathsf{k}^2 - k^2)\,, \tag{2.5}$$

where $k = k(\mathbf{x})$ is determined by (1.7). Introducing the truncated expansion

$$\Phi(\mathbf{x},z) = \{\mathsf{F}(k^2,z) - (\partial\mathsf{F}/\partial\mathsf{k}^2)_{\mathsf{k}=k}\mathsf{H} + O(\mathsf{H}^2)\}\Phi_0(\mathbf{x})\,, \tag{2.6}$$

invoking

$$\mathsf{H}\Phi_0 = -H^{-1}(\nabla H\cdot\nabla\Phi_0) + O(\sigma^2\Phi_0)\,, \tag{2.7}$$

where H is given by (1.10), and evaluating F and $\partial\mathsf{F}/\partial\mathsf{k}^2$ through (2.4), we obtain

$$\Phi(\mathbf{x},z) = [F(h,z) + G(h,z)(\nabla h\cdot\nabla) + O(\sigma^2)]\Phi_0(\mathbf{x})\,, \tag{2.8}$$

where $F = \dfrac{\cosh k(z+h)}{\cosh kh}$, $G = \dfrac{1}{2}\left[\dfrac{kz \sinh k(z+h) - \sinh kh \sinh kz}{k^2 \cosh kh}\right] \dfrac{dH/dh}{H}$.

(2.9a,b)

2.2 Truncated Lagrangian

We now adopt (2.8) as a trial function in (2.3) and introduce the abbreviations

$$\langle(\ )\rangle \equiv \int_{-h}^{0} (\ )dz \quad \text{and} \quad \Psi \equiv \nabla h \cdot \nabla \Phi_0 \qquad (2.10a,b)$$

to obtain

$$\mathsf{L} = -\kappa |\Phi_0|^2 + \langle |\nabla(F\Phi_0 + G\Psi)|^2 + |F_z\Phi_0 + G_z\Psi|^2\rangle . \qquad (2.11)$$

Invoking $|(\ )|^2 \equiv (\ )(\ )^*$, where $(\ )^*$ is the complex conjugate of $(\ )$,

$$\nabla F = F_h \nabla h \ , \quad \langle F^2\rangle = H \ , \quad \langle F_z^2\rangle = \kappa - k^2 H \quad \text{and} \quad \langle F_z G_z\rangle = -k^2\langle FG\rangle \ , \qquad (2.12a\text{-}d)$$

where H is given by (1.10), transforming the terms in $\Phi_0^*(\nabla h \cdot \nabla\Psi)$ and $\Psi^*(\nabla h \cdot \nabla\Psi)$ through Green's theorem and terms like $\Phi_0^*\nabla\Phi_0$ through integration by parts, and discarding a pure divergence (which makes no contribution to the variation $\delta\bar{L}$), we obtain

$$\mathsf{L} = \mathsf{L}_{ms} + K|\Phi_0|^2 + M|\Psi|^2 + \langle FG\rangle(\nabla\Phi_0^* \cdot \nabla\Psi + \nabla\Phi_0 \cdot \nabla\Psi^*) + \langle G^2\rangle |\nabla\Psi|^2 , \qquad (2.13)$$

where

$$\mathsf{L}_{ms} = H(|\nabla\Phi_0|^2 - k^2|\Phi_0|^2) \qquad (2.14)$$

is the mild-slope approximation to L,

$$K = \langle F_h^2\rangle(\nabla h)^2 - \nabla\cdot\{[\langle FF_h - k^2 FG + F_h G_h(\nabla h)^2\rangle - \nabla\cdot(\langle F_h G\rangle h')]\nabla h\} \qquad (2.15a)$$

and

$$M = \langle G_z^2\rangle + 2\langle FG_h - F_h G\rangle + \langle G_h^2\rangle(\nabla h)^2 - \nabla\cdot(\langle GG_h\rangle\nabla h) . \qquad (2.15b)$$

The retention of all terms in (2.13) leads to a fourth-order partial differential equation. CP's modified mild-slope approximation follows from the neglect of all terms in G , which reduces K to (1.14) and (2.13) to

$$\mathsf{L} = \mathsf{L}_{ms} + K|\Phi_0|^2 = H|\nabla\Phi_0|^2 - (k^2 H - K)|\Phi_0|^2 . \qquad (2.16)$$

3. Quasi-geometrical-optics approximation

The geometrical-optics approximation

$$\Phi_0 = A\,(kH)^{-1/2}\,e^{i\theta}\,, \quad (\nabla\theta)^2 = k^2(\mathbf{x})\,, \tag{3.1a,b}$$

to the solution of the mild-slope equation (1.9), where A is a constant and kH is the dimensionless group velocity (1.10), suggests the transformation

$$\Phi_0(\mathbf{x}) = (kH)^{-1/2}E(\theta)\,. \tag{3.2}$$

We relegate further discussion of two-dimensional waves to Appendix A and, here and in §4, assume $h = h(x)$ and replace $\nabla(\,)$ by $(\,)'$ and (2.2) by

$$\bar{L} = \tfrac{1}{4}\int \hat{\mathsf{L}}\,d\theta\,, \quad \hat{\mathsf{L}} \equiv k^{-1}\mathsf{L}\,, \quad \theta(x) = \int_0^x k(\xi)\,d\xi\,. \tag{3.3a-c}$$

Substituting (3.2) into (2.13) and integrating the term in $\partial|E|^2/\partial\theta$ by parts, we obtain

$$\hat{\mathsf{L}} = \hat{\mathsf{L}}_{ms} + (k^2H)^{-1}K\,|E|^2 + P\,|E_\theta|^2 + k^2H^{-1}\langle G^2\rangle h'^2|E_{\theta\theta}|^2 + O(\sigma^3)\,, \tag{3.4}$$

where
$$\hat{\mathsf{L}}_{ms} = |E_\theta|^2 - (1 - Q_{ms})|E|^2\,, \tag{3.5}$$
is the mild-slope approximation to $\hat{\mathsf{L}}$,

$$Q_{ms} = k^{-1}(\Gamma h')' + (\Gamma h')^2\,, \quad \Gamma = \tfrac{1}{2}(k^2H)^{-1}(dkH/dh) = \tfrac{1}{4}(kH)^{-2}T(1-T^2)(1-khT)\,, \tag{3.6a,b}$$

$$K = \langle F_h^2\rangle h'^2 - (\langle FF_h - k^2FG\rangle h')'\,, \tag{3.7}$$

$$P = H^{-1}[\langle FG\rangle h'' - \langle FG\rangle_h h'^2 + \langle 2FG_h - 2F_hG + G_z^2\rangle h'^2] + O[(h'^2)'']\,, \tag{3.8}$$

and F and G are given by (2.9). Anticipating (3.11), which implies $E_{\theta\theta} = -E[1 + O(\sigma)]$, we reduce (3.4) to

$$\hat{\mathsf{L}} = (1+P)|E_\theta|^2 - (1-Q)|E|^2 + O(\sigma^3)\,, \tag{3.9}$$

where
$$Q = Q_{ms} + (k^2H)^{-1}(K + k^4\langle G^2\rangle h'^2)\,, \tag{3.10}$$

and, here and subsequently, we regard P and Q as functions of θ. Hamilton's principle, $\delta\hat{\mathsf{L}}/\delta E = 0$, then implies

$$E_{\theta\theta} + E = QE - (PE_\theta)_\theta \,. \tag{3.11}$$

Following Liouville (Erdélyi 1956, §4.1) we transform (3.11) to

$$E(\theta) = A_+ e^{i\theta} + A_- e^{-i\theta} + \int_0^\theta [Q(\hat\theta)E(\hat\theta)\sin(\theta-\hat\theta) - P(\hat\theta)E'(\hat\theta)\cos(\theta-\hat\theta)]d\hat\theta \,, \tag{3.12}$$

wherein A_+ and A_- are complex amplitudes, and $h = h_0 =$ constant for $x < 0$. It is convenient to write the solution of (3.12) as $E(\theta) = A_+ E_+(\theta) + A_- E_+^*(\theta)$ where

$$E_+(\theta) = e^{i\theta} + \int_0^\theta [Q(\hat\theta)E_+(\hat\theta)\sin(\theta-\hat\theta) - P(\hat\theta)E'_+(\hat\theta)\cos(\theta-\hat\theta)]d\hat\theta \,. \tag{3.13}$$

Equation (3.13) may be solved by iteration starting from the function $e^{i\theta}$. The next approximation admits the form

$$E_+(\theta) = e^{i\theta} + \tfrac{1}{2} i \int_0^\theta \{[Q(\hat\theta) - P(\hat\theta)]\, e^{2i\hat\theta - i\theta} - [Q(\hat\theta) + P(\hat\theta)]\, e^{i\theta}\} d\hat\theta + O(Q^2) \,. \tag{3.14}$$

We refer to the first two terms on the right-hand side of (3.14) as the *quasi-geometrical optics* approximation to E_+. The iteration used here is discussed further in §4.1.

We recover: (i) the geometrical-optics approximation by neglecting P and Q; (ii) the quasi-geometrical-optics reduction of the mild-slope approximation by neglecting P and approximating Q by Q_{ms} (3.6); (iii) the quasi-geometrical-optics reduction of the modified mild-slope approximation by neglecting all terms in G, which implies the neglect of P and the approximation of K by (1.14) in (3.10) and yields

$$Q = Q_{ms} + (k^2 H)^{-1} K \equiv k^{-1} Q_1 h'' + Q_2 h'^2 \,, \tag{3.15a}$$

where

$$Q_1 = \Gamma + (kH)^{-1} K_1 = \tfrac{1}{2} \frac{(1-T^2)}{kh(1-T^2)+T} = \tfrac{1}{2} \frac{d}{dh}\left(\frac{1}{k}\right) \tag{3.15b}$$

and

$$\begin{aligned} Q_2 &= \Gamma^2 + k^{-1}\Gamma_h + (kH)^{-1}K_2 \\ &= -\tfrac{1}{2}(1-T^2)^2(2kH)^{-4}[\tfrac{2}{3}(kh)^4(1-T^2)^2 + \tfrac{8}{3}(kh)^3 T(1-T^2) \\ &\quad + (kh)^2(1+T^2)^2 - 2khT^3 + T^2] \,. \end{aligned} \tag{3.15c}$$

Letting $kh \to (\kappa h)^{1/2} \to 0$, we obtain the shallow-water limit

$$Q \to Q_{ms} \to \tfrac{1}{4}\kappa^{-1}(h'' - \tfrac{1}{4}h^{-1}h'^2)\,. \tag{3.16}$$

Figure 1 shows the effect of approximating Q_1 and Q_2 in both of the ways described above. In figure 1a Q_1 is plotted against kh as a solid line; the mild-slope approximation to Q_1, found from (3.6), and the modified mile-slope approximation to Q_1 (3.15b) are given as dotted and broken lines respectively. Figure 1b is as figure 1a, but for Q_2 rather than Q_1. It is clear that Q_1 and Q_2 are qualitatively similar to their approximations; further evidence in support of these approximations is given in §§5 and 6.

4. Topographic reflection

We apply the results of §3 to the reflection of a straight-crested wave on the assumptions that: P is negligible; h is constant in $x < 0$ and $x > \ell$; $h(x)$ and $h'(x)$ are continuous in $0 < x < \ell$, but $h'(x)$ may be discontinuous at $x = 0$ and ℓ. Positing

$$E(\theta) = e^{i\theta} + Re^{-i\theta}\,, \quad \theta = k_0 x \quad (x < 0) \tag{4.1}$$

for an incident wave of normalized complex amplitude $\equiv 1$ and setting $A_+ = 1$, $A_- = R$ and $P = 0$, we reduce (3.12) to

$$E(\theta) = e^{i\theta} + Re^{-i\theta} + \int_{0-}^{\theta} Q(\hat{\theta})E(\hat{\theta})\sin(\theta - \hat{\theta})\,d\hat{\theta}\,, \tag{4.2}$$

in which the lower limit of 0– allows for a possible discontinuity in h'. The radiation condition that the left-moving wave be absent in $x > \ell$ implies (here and except in §4.1 the limits 0 and θ_1 are implicitly 0– and θ_1+)

$$R = -\tfrac{1}{2}i\int_{0}^{\theta_1} Q(\theta)E(\theta)e^{i\theta}d\theta\,, \quad \theta_1 \equiv \theta(\ell)\,, \tag{4.3a,b}$$

which permits the reduction of (4.2) to

$$E(\theta) = e^{i\theta} - \tfrac{1}{2}i\int_0^{\theta_1} Q(\hat{\theta})E(\hat{\theta})\exp(i|\theta-\hat{\theta}|)\,d\hat{\theta}\,. \tag{4.4}$$

Either (4.2), subject to the constraint (4.3), or (4.4) may be solved by iteration, starting from the first approximation $E = e^{i\theta}$. The corresponding first (quasi-geometrical-optics) and second approximations to R are

$$R_1 = -\tfrac{1}{2}i\int_0^{\theta_1} Q(\theta)e^{2i\theta}d\theta \tag{4.5}$$

and
$$R_2 = R_1 - \tfrac{1}{4}\int_0^{\theta_1}\int_0^{\theta_1} Q(\theta)Q(\hat{\theta})\exp[2i\max(\theta,\hat{\theta})]\,d\theta d\hat{\theta} \tag{4.6a}$$

$$= R_1 - \tfrac{1}{4}\int_0^{\theta_1} Q(\theta)e^{2i\theta}d\theta\int_0^{\theta} Q(\hat{\theta})d\hat{\theta} - \tfrac{1}{4}\int_0^{\theta_1} Q(\theta)d\theta\int_{\theta}^{\theta_1} Q(\hat{\theta})e^{2i\hat{\theta}}d\hat{\theta} \tag{4.6b}$$

$$= R_1 - \tfrac{1}{2}\int_0^{\theta_1} Q(\theta)e^{2i\theta}d\theta\int_0^{\theta} Q(\hat{\theta})d\hat{\theta}\,, \tag{4.6c}$$

where (4.6c) follows from (4.6b) through the interchange of θ and $\hat{\theta}$ in the second double integral in (4.6b) or, equivalently, from the symmetry of the double integrand in (4.6a) with respect to the diagonal $\hat{\theta} = \theta$.

4.1 Neumann-series solution

Under our present assumption that P may be neglected (3.13) can be written as the Volterra integral equation

$$E_+(\theta) = e^{i\theta} + \int_{0+}^{\theta} Q(\hat{\theta})\sin(\theta-\hat{\theta})E_+(\hat{\theta})d\hat{\theta}\,, \tag{4.7}$$

which may be solved using a Neumann series. (Here the lower integration limit is $0+$; contributions due to possible discontinuities in h' are dealt with in (4.8) below.) Let $E_+^{(0)}(\theta) = e^{i\theta}$, the free term in (4.7), so that the partial sums of the Neumann series for E_+ are $E_+^{(n)}$, where

$$E_+^{(n)}(\theta) = e^{i\theta} + \int_0^{\theta} Q(\hat{\theta})\sin(\theta-\hat{\theta})E_+^{(n-1)}(\hat{\theta})d\hat{\theta}$$

$n = 1,2,3,\cdots$. [The convergence of $E_+^{(n)}$ to the solution E_+ as $n \to \infty$ is guaranteed when Q is bounded (see Porter & Stirling (1990, pp. 81 *et seq.*)). The function Q is unbounded only when $kh \downarrow 0$ (see figure 1), a limit which is precluded in the present analysis.] In practice we find that the convergence is rapid and that $E_+^{(n)}$ is a good approximation to E_+, even for small values of n .

We now use (4.1) and the fact that there are only right-moving waves in $x > \ell$ to deduce that

$$\left.\begin{aligned} E_\theta(0+) + [\mathrm{i} - Q_{10}h'(0+)]E(0) = 2\mathrm{i} \\ E_\theta(\theta_1-) - [\mathrm{i} + Q_{11}h'(\ell-)]E(\theta_1) = 0 \end{aligned}\right\}, \tag{4.8}$$

in which $Q_{10} \equiv Q_1(\theta_0)$ and $Q_{11} \equiv Q_1(\theta_1)$. (The terms involving Q_{10} and Q_{11} are required to take account of the assumed discontinuities in h'.) Now $E = A_+E_+ + A_-E_+^*$, and therefore (4.8) form a pair of equations for $A_\pm$ in terms of point values of E_+ and $E_{+\theta}$. It follows that $E_+^{(n)}$ gives rise to $A_\pm^{(n)}$ approximating $A_\pm$. This, in turn, leads to the approximation

$$R_n = A_+^{(n)}E_+^{(n)}(0) + A_-^{(n)}E_+^{(n)*}(0) - 1 = A_+^{(n)} + A_-^{(n)} - 1 \,. \tag{4.9}$$

It is readily seen that if $n = 1$ in (4.9) we obtain the approximation (4.5), and $n = 2$ gives (4.6a,b). The approach described here makes clear how subsequent approximations can be derived and also provides a framework in which convergence of the iteration is guaranteed.

4.2 Variational formulation

Multiplying (4.4) by kQE , integrating over $(0-, \ell+)$, and dividing the result by the square of (4.3), we obtain

$$\frac{1}{R} = \frac{2\mathrm{i}\int QE^2 d\theta - \iint (QE)(\hat{Q}\hat{E})\exp(\mathrm{i}\,|\theta - \hat{\theta}\,|)\,d\hat{\theta}\,d\theta}{(\int QE e^{\mathrm{i}\theta} d\theta)^2}\,, \tag{4.10}$$

in which the limits of integration are 0– and θ_1+, and the double integrand is symmetric in θ and $\hat{\theta}$. This quadratic form is stationary with respect to first-order variations about the solution of (4.4) and invariant under a scale change of E. For example, the trial function $E = e^{i\theta}$ yields the variational approximation

$$\frac{1}{R_v} = \frac{1}{R_1} + \frac{R_1 - R_2}{R_1^2} \tag{4.11a}$$

$$= \frac{1}{R_2}\left[1 - \left(\frac{R_1 - R_2}{R_1}\right)^2\right], \tag{4.11b}$$

where R_1 and $R_1 - R_2$ are given by (4.5) and (4.6). The error in (4.11), which is second order in the error in the trial function, is of the same order as that in R_2, but the variational approximation appears to be superior to the second-order approximation (4.6) if $|R|$ is not small; see, e.g., §6.

The variational form (4.10) could be used to construct systematic approximations to R through an appropriate expansion of E; however, this procedure does not appear to offer any advantage over that of §4.1.

4.3 Interpolation of E

We obtain a collocation approximation through the interpolation

$$E = \frac{E_0 \sin(\theta_1 - \theta) + E_1 \sin\theta}{\sin\theta_1} \quad (\sin\theta_1 \neq 0), \tag{4.12}$$

wherein the subscript 0/1 implies evaluation at $x = 0/\ell$. Substituting (4.12) into (4.4) and setting $x = 0$ and $x = \ell$, we obtain a pair of linear algebraic equations in E_0 and E_1, the solution of which yields

$$DE_0 = s_1 + \tfrac{1}{2} e_1(2I - J - \bar{J}), \quad DE_1 = e_1 s_1 + \tfrac{1}{2}[(1 + e_1^2)I - J - \bar{J}e_1^2], \tag{4.13a,b}$$

where $$D = s_1 + Ie_1 - \tfrac{1}{2}(J\bar{e}_1 + \bar{J}e_1) + \tfrac{1}{2} ie_1(I^2 - |J|^2), \tag{4.14}$$

$$e_1 \equiv e^{i\theta_1}, \quad s_1 \equiv \sin\theta_1, \tag{4.15a,b}$$

$$I = \tfrac{1}{2}\int Q d\theta, \quad J = \tfrac{1}{2}\int Q e^{2i\theta} d\theta = iR_1, \tag{4.16a,b}$$

and $\overline{(\,)}$ is the complex conjugate of $(\,)$. Invoking (4.1) at $x = 0$, we obtain

$$R_E = E_0 - 1 = -iD^{-1}[Js_1 + \tfrac{1}{2} e_1(I^2 - |J|^2)] \tag{4.17}$$

for the corresponding approximation to the reflection coefficient. This approximation appears to be as good as either (4.6) or (4.11) if $\sin\theta_1$ is not too small and avoids the double integral in (4.6). However, although the indeterminacy associated with $\sin\theta_1 = 0$ can be resolved, the approximation is poor for $|\sin\theta_1| \ll 1$.

5. Booij's ramp

As a first example, we consider the linear ramp described by

$$h = \begin{matrix} h_0 & (x \le 0) \\ h_0 - \sigma x & (0 \le x \le \ell), \\ h_1 & (x \ge \ell) \end{matrix} \qquad \sigma \equiv \frac{h_0 - h_1}{\ell}, \tag{5.1a,b}$$

for which (3.15a) and (4.13a,b) may be reduced to

$$Q = \sigma k^{-1}[-Q_{10}\delta(x) + Q_{11}\delta(\ell - x)] + \sigma^2 Q_2(x), \tag{5.2}$$

$$I = \tfrac{1}{2}\sigma(Q_{11} - Q_{10}) + \sigma^2 I_2, \quad J = \tfrac{1}{2}\sigma(Q_{11}e_1^2 - Q_{10}) + \sigma^2 J_2, \tag{5.3a,b}$$

where
$$[I_2, J_2] = \tfrac{1}{2}\int Q_2[1, e^{2i\theta}]d\theta. \tag{5.4}$$

The phase integral may be placed in the form

$$\theta = \int_0^x k dx = \frac{1}{\sigma}\int_{kh}^{k_0 h_0}\left[1 + \frac{2\hat{k}}{\sinh 2\hat{k}}\right]d\hat{k} \equiv \frac{\Theta(kh)}{\sigma}, \tag{5.5}$$

the substitution of which into (5.4) yields

$$[I_2, J_2] = \frac{1}{2\sigma}\int_{k_1 h_1}^{k_0 h_0} Q_2(\hat{k})\left[1 + \frac{2\hat{k}}{\sinh 2\hat{k}}\right][1, e^{2i\theta}]d\hat{k}. \tag{5.6}$$

$J_2 = O(1)$ if $\sigma \ll 1$, by virtue of which (4.5) may be approximated by

$$R_1 = \tfrac{1}{2} \mathrm{i} \sigma (Q_{10} - Q_{11} e^{2\mathrm{i}\theta_1}) + O(\sigma^2) \quad (\sigma \to 0). \tag{5.7}$$

The linear ramp problem has been solved by Booij (1983) and Porter & Staziker (1995) through numerical integration of the mild-slope equation and modified mild-slope equation, respectively, for $\kappa h_{0,1} = 0.6/0.2$, which imply $kh = 0.861/0.463$. The corresponding values of Q_{10}, Q_{11} and θ_1 are 0.226, 0.503 and $0.698/\sigma$, the substitution of which into (5.7) yields

$$|R| = 0.275\sigma[1 - 0.748\cos(1.40/\sigma)]^{1/2} + O(\sigma^2). \tag{5.8}$$

The corresponding mild-slope approximation, for which Q_1 is given by Γ(3.6b), is

$$|R| = 0.223\sigma[1 - 0.482\cos(1.40/\sigma)]^{1/2} + O(\sigma^2), \tag{5.9}$$

in agreement with Miles & Zou (1993). These approximations, and others described in §4, are compared with the results of Booij and Porter & Staziker in figures 2 and 3, where the reflection coefficient is plotted against the dimensionless parameter $\kappa\ell$.

For the purposes of comparison we have computed reflection coefficients from direct integrations of the mild-slope and modified mild-slope equations. These are denoted R_{ms} and R_{mms} respectively.

In figure 2 we consider the mild-slope approximation. The solid line shows values of $|R_{ms}|$, and the crosses correspond to Booij's results for the full equations (read from Booij's paper using eye and ruler). The dotted line shows the approximation given by equation (5.9), and it is clear that these results are reliable for $\kappa\ell (= 0.4/\sigma) > 1$. There are three dotted lines shown, all appearing on the left of the graph near $|R| \approx 0.4$. These curves show the approximations $|R_1|$, $|R_2|$ and $|R_E|$ described in §4 and are nearly indistinguishable. (Note that $|R_E|$ is not shown near $\sin\theta_1 = 0$, where we know the approximation to be poor; this occurs near the three local minima of $|R_{ms}|$.) As indicated by the fact that $R_2 \approx R_1$ here, the iteration described in §4.1 converges to a curve in agreement with the broken lines.

Figure 3 has the same format as figure 2, but the modified mild-slope (rather than the mild-slope) equation has been used. The dotted line, corresponding to (5.8), is clearly reliable for $\kappa\ell > 1$, and the E-interpolation produces good approximations everywhere except near $\sin\theta_1 \approx 0$, where it has not been implemented. The curves corresponding to $|R_1|$, $|R_2|$, $|R_E|$ and $|R_{mms}|$ lie on top of one another, and broken lines are only visible to the extreme left of the graph. It is evident that the modified mild-slope equation, which more consistently deals with terms involving h' and h'', enables the quasi-geometrical optics approach to produce excellent approximations.

For smaller values of $\kappa\ell$, not shown on figure 3, $|R_1 - R_{mms}|$ achieves a maximum value of almost 0.5, but $|R_2 - R_{mms}|$ is never greater than 0.0019. We note that, where R_1 and R_2 differ significantly, R_E is always a better approximation than R_1, in fact $|R_E - R_{mms}|$ has a maximum value less than 0.15.

In both figures 2 and 3 R_2 and R_n $(n > 2)$ are indistinguishable to the eye, for which reason we have not included R_v (an approximation of the same order as R_2). Values of R_v are given for another test problem considered in the next section.

6. Ripple bed

As a second example, we consider the ripple bed described by [Davies & Heathershaw (1984) after shifting the origin of x and replacing their ℓ by $\alpha \equiv 2n\pi/\ell$ in the present notation]

$$h = \begin{cases} h_0 & (x \le 0) \\ h_0 - b\sin\alpha x & (0 \le x \le \ell) \\ h_0 & (x \ge \ell) \end{cases} \quad (6.1)$$

on the assumption that $b/h_0 \ll 1$. Substituting (6.1) into (3.15a), we obtain (cf. (5.2))

$$Q = \alpha b\{(Q_1/k)_0[-\delta(x)+\delta(\ell-x)] + (Q_1/k)\alpha\sin\alpha x\} + \alpha^2 b^2 Q_2(x)\cos^2\alpha x\ , \quad (6.2)$$

the substitution of which into (4.5), followed by the expansion of k and Q about $x = 0$ and the invocation of $dk/dh = -2k^2Q_1$ (3.15b), yields

$$R_1 = 4k_0^2\alpha b Q_{10}(4k_0^2 - \alpha^2)^{-1}e^{ik_0\ell}\sin k_0\ell + O(\alpha^2b^2)\ , \quad (6.3)$$

in agreement with Davies & Heathershaw's (25). The corresponding approximation to the Bragg-resonant peak of $|R|$ is

$$|R_1|_{\max} = \tfrac{1}{4}\alpha^2 b\ell Q_{10}[1 + O(\alpha^2b^2)] \quad (2k_0 = \alpha)\ . \quad (6.4)$$

Figure 4 shows approximations to $|R|$ for $b = 0.16h_0$ and $n = 10$. Here we have used the modified mild-slope equation, since it is known that the mild-slope equation performs poorly for this test problem (see, for example, CP). The solid line corresponds to $|R_{mms}|$; the dotted, dash-dot and dashed curves show $|R_1|$, $|R_2|$ and $|R_3|$, respectively. Curves for $|R_n|$ with $n \ge 4$ are identical (to the eye) to the solid line. Once again we see that the quasi-geometrical approximation performs exceptionally well when $|R|$ is small, the curve for R_1 being very close to the solid curve. Only when $|R|$ is large do we require further approximations, and even in the places where $|R| > 0.7$, we see that very few iterations are required, R_3 being sufficient everywhere.

A portion of the curve corresponding to R_v, as given by (4.11), is indicated on figure 4 by triangles. (Away from the principal peak R_v is indistinguishable from R_2 and is not shown.) We see that, where reflection is large, and R_2 differs significantly from R_3, the variational formulation gives better approximations to R than does R_2, even though the two estimates are of the same order of accuracy when small.

7. Conclusions

It follows from the preceding results that R_1, the quasi-geometrical approximation to the reflection coefficient based on the modified mild-slope equation, is remarkably accurate when reflection is weak. In parametric domains where reflection is stronger, a means has been described to generate increasingly accurate approximations (R_n , $n > 1$).

Two further approximations have been discussed: R_E (which is valid away from $\sin\theta_1 = 0$) and R_v (a variational approximation). In all of the computations that have been carried out it has been found that R_E (when valid) is superior to R_1 but inferior to R_2, whereas R_v is better than R_2 but worse than R_3. (That these comparisons are not evident on all of figures 2, 3 and 4 is due to the fact that convergence of the sequence (R_n) is often so rapid that, as far as the eye can tell, $R_1 = R_E = R_2 = R_v$.) The approximations R_E and R_v are of practical use since R_E is cheaper to calculate that R_2 and R_v is cheaper to find than R_3.

This work was supported in part by National Science Foundation Grant OCE95-01508 and by Office of Naval Research Grant N00014-92-J-1171.

Appendix A. Quasi-geometrical-optics approximation: two-dimensional topography

The extension of the quasi-geometrical-optics approximation of §3 for two-dimensional topography begins with the solution of the eikonal equation (3.1b) for $\theta = \theta(\mathbf{x})$ and

$$\mathbf{k} = \nabla\theta \equiv k\,[\mu, \nu]\,, \quad \mu^2 + \nu^2 = 1\,, \tag{A1a,b}$$

where μ and ν are the direction cosines of the vector $\mathbf{k}$. Assuming that this solution has been determined, we adopt the orthogonal coordinates θ and s through the transformation

$$d\theta = k(\mu dx + \nu dy)\,, \quad ds = -\nu dx + \mu dy\,, \tag{A2a,b}$$

for which the Jacobian is k, and replace (3.3a,b) by

$$\hat{\mathcal{L}} = \tfrac{1}{4}\rho \iint \hat{\mathsf{L}}\, d\theta\, ds\,, \quad \hat{\mathsf{L}} = k^{-1}\mathsf{L}\,. \tag{A3a,b}$$

Substituting (3.2) into (2.11) and proceeding as in §3, we obtain (after a nontrivial reduction) $\hat{\mathsf{L}}$ in the form (3.9) with

$$P = N/H\,, \quad Q = (\Gamma\lambda)_\theta + (\Gamma\nabla h)^2 + (k^2 H)^{-1}(K + k^4\langle G^2\rangle h'^2)\,, \tag{A4a,b}$$

where
$$K = \langle F_h^2\rangle(\nabla h)^2 - \nabla\cdot(\langle FF_h - k^2 FG\rangle\nabla h)\,, \tag{A5a}$$

$$N = 2\Gamma\langle FG\rangle k\,[\lambda^2 - (\nabla h)^2] + k\,[\lambda_\theta\langle FG\rangle - \lambda\langle FG\rangle_\theta] + \lambda^2\langle 2FG_h - 2F_h G + G_z^2\rangle\,, \tag{A5b}$$

$$k\,\partial_\theta = \mu\partial_x + \nu\partial_y\,, \quad \lambda = \mu h_x + \nu h_y\,, \tag{A6a,b}$$

and F, G and Γ are given by (2.9a,b) and (3.6b).

REFERENCES

Booij, N. 1983 A note on the accuracy of the mild-slope equation. *Coastal Eng*. **7**, 191–203.

Chamberlain, P. G. & Porter, D. 1995 The modified mild-slope equation. *J. Fluid Mech*. **291**, 393–407 (abbreviated as CP in text).

Davies, A. G. & Heathershaw, A. D. 1984 Surface-wave propagation over sinusoidally varying topography. *J. Fluid Mech.* **144**, 419–443.

Erdélyi, A. 1956 *Asymptotic Expansions*. Dover.

Keller, J.B. 1958 Surface waves on water of non-uniform depth. *J. Fluid Mech.* **4**, 607-614.

Mei, C. C. 1983 *The Applied Dynamics of Ocean Surface Waves*. Wiley-Interscience.

Miles, J. 1985 Surface waves in water of variable depth. *J. Fluid Mech*. **152**, 379–389.

Miles, J. & Zou, Q-P 1993 Gravity-wave reflection at a discontinuity in bottom slope. *J. Phys. Ocean*. **23**, 1870–71.

Porter, D. & Staziker, D. J. 1995 Extensions of the mild-slope equation. *J. Fluid Mech.* **300**, 367–382.

Porter, D. & Stirling, D.S.G. 1990 *Integral Equations*. Cambridge University Press.

Smith, R. & Sprinks, T. 1975 Scattering of surface waves by a conical island. *J. Fluid Mech.* **72**, 373–384.

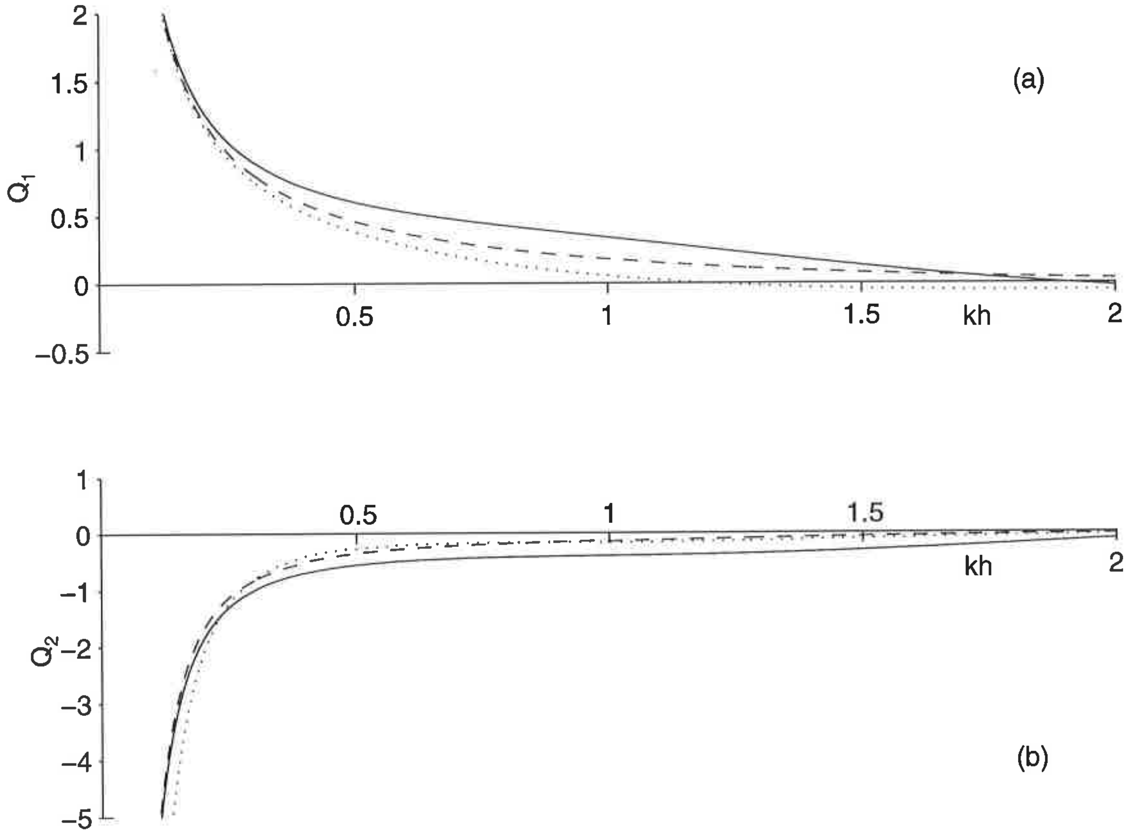

Figure 1: The functions Q_1 and Q_2 plotted against kh. The mild-slope and modified mild-slope approximations to Q_1 and Q_2 are shown as dotted and broken lines respectively.

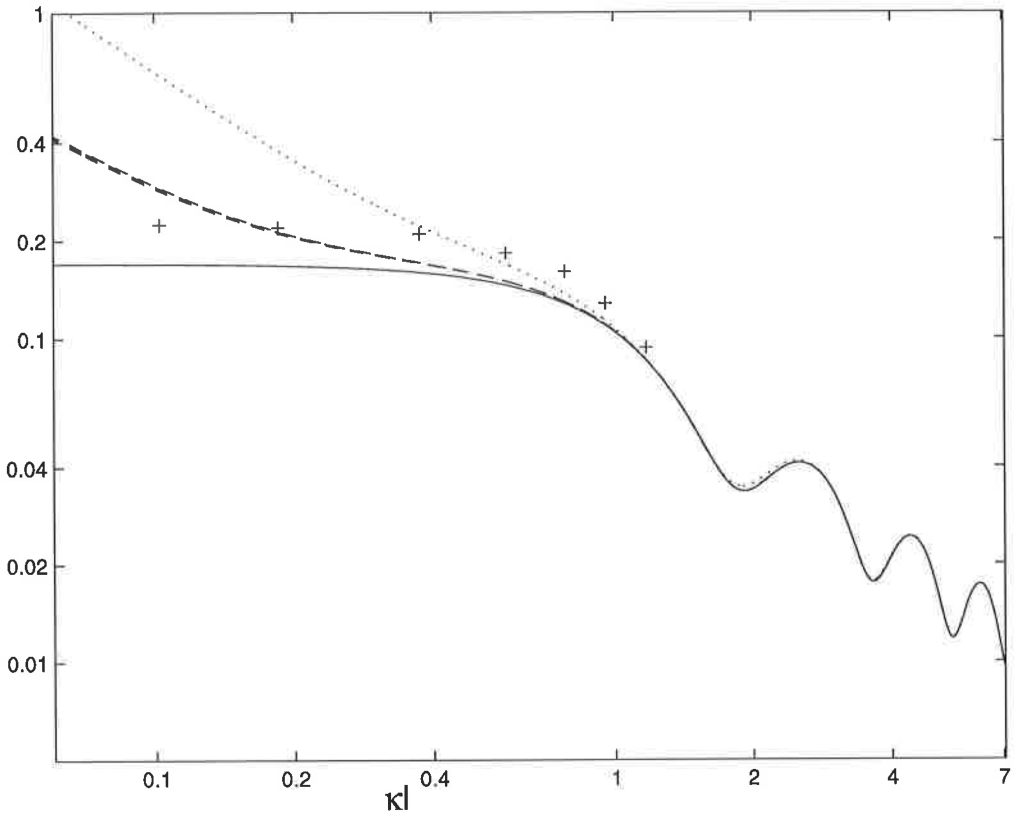

Figure 2: Approximations to $|R|$ plotted against $\kappa\ell$. The crosses are from Booij's solution of the full problem, the solid line shows $|R_{ms}|$, the dotted line shows the approximation (5.9) and the broken lines show R_1, R_2 and R_E each calculated using (3.6) to approximate Q.

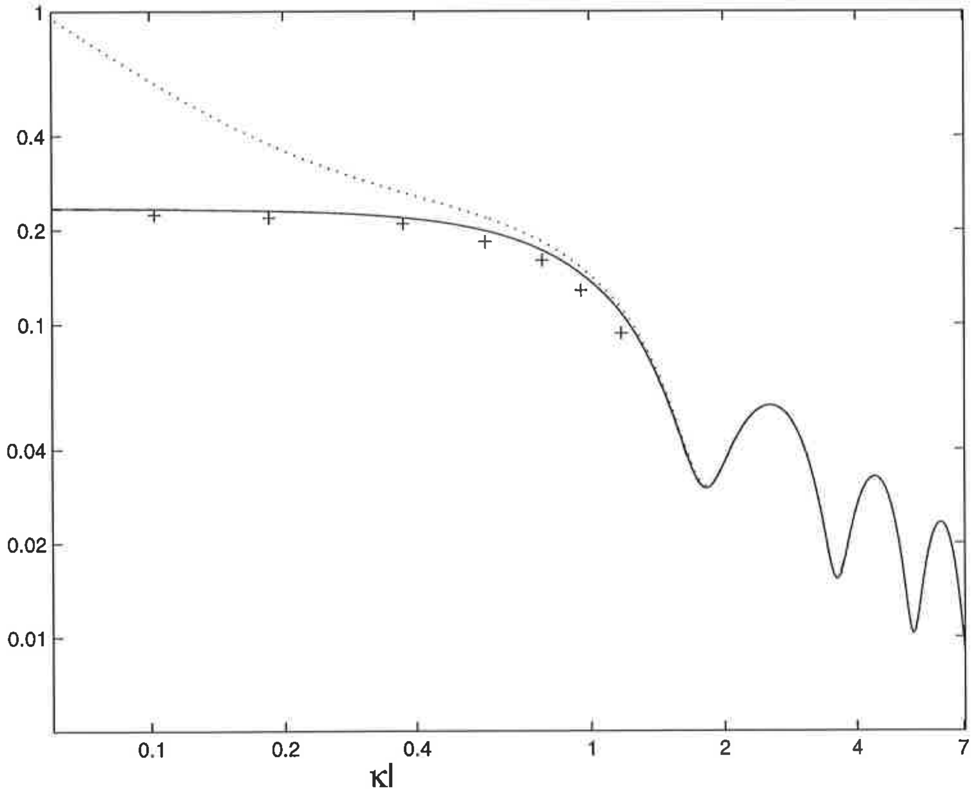

Figure 3: Approximations to $|R|$ plotted against $\kappa\ell$. The crosses are from Booij's solution of the full problem, the solid line shows $|R_{mms}|$, the dotted line shows the approximation (5.8) and the broken lines (which coincide with the solid line everywhere except near the far left of the graph) show R_1, R_2 and R_E each calculated using (3.15) to approximate Q.

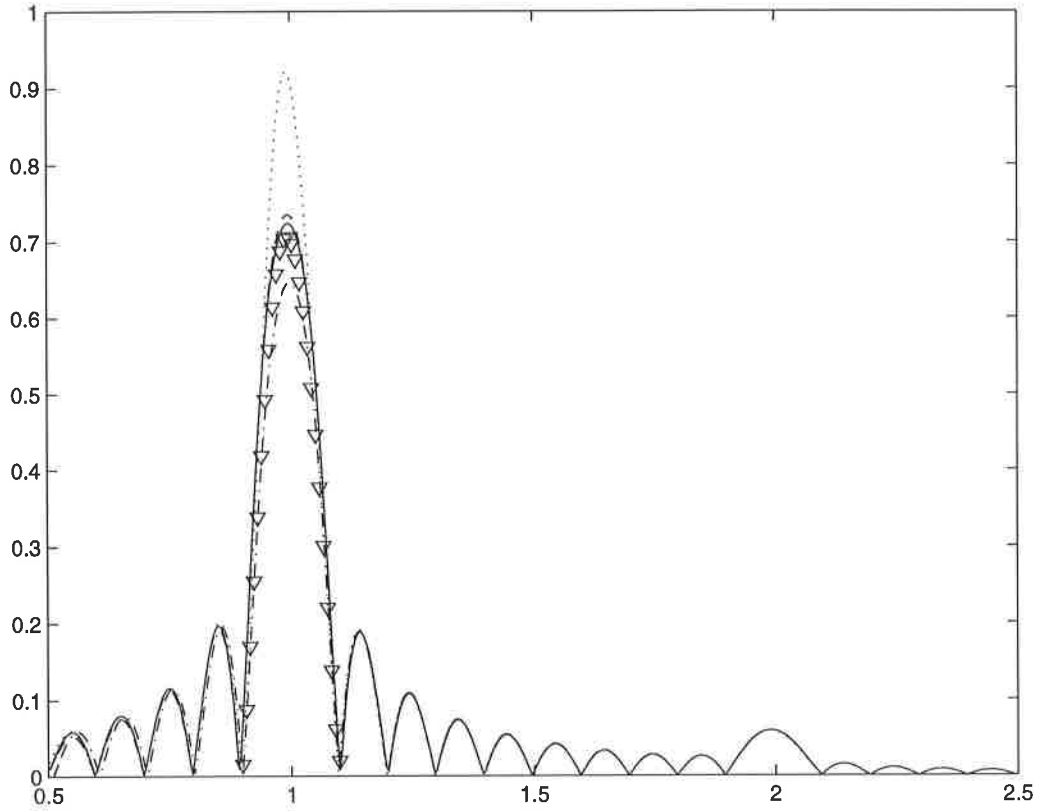

Figure 4: Approximations to $|R|$ for the ripple-bed test problem. The solid line shows $|R_{mms}|$; the dotted, dash-dot and dashed lines show $|R_1|$, $|R_2|$ and $|R_3|$ respectively. A portion of the variational approximation $|R_v|$ is shown as triangles.